

**EFFECT OF VARIABLE VISCOSITY, ACTIVATION ENERGY AND
IRREGULAR HEAT SOURCES ON CONVECTIVE HEAT AND MASS
TRANSFER FLOW OF NANOFLUID IN A CHANNEL WITH
BROWNIAN MOTION AND THERMOPHORESIS**

¹Dr. K. Satya Narayana and ^{2*}Dr. G. N. Ramakrishna

¹Associate Professor in Mathematics, Sri Venkateswara Institute of Technology, Anantapur –
515 001, A.P., India.

²Assistant Professor in Mathematics, S.S.B.N. Degree College (Autonomous), Anantapur –
515 001, A.P., India.

Article Received on 29/11/2022

Article Revised on 19/12/2022

Article Accepted on 09/01/2023

***Corresponding Author**

Dr. G.N. Ramakrishna

Assistant Professor in
Mathematics, S.S.B.N.
Degree College
(Autonomous), Anantapur –
515 001, A.P., India.

ABSTRACT

In this analysis an attempt has been made to investigate the effect of Brownian motion and thermophoresis effect on convective heat and mass transfer flow of nanofluid in a vertical channel with variable viscosity and activation energy in the presence of non-uniform heat sources. The non linear coupled equations have been solved by Runge-Kutta Fehlberg method considering shooting techniques. It is found

that an increase in viscosity parameter (B) enhances the velocity, temperature and reduces nanoparticle concentration velocity and temperature reduces with E_1 and depreciates with δ . Nano concentration augments with E_1 and decays with δ .

KEYWORDS: Nano fluid, Brownian motion, Thermophoresis, activation energy, non-uniform heat sources and vertical channel.

1. INTRODUCTION

The vertical channel is an often encountered configuration in thermal engineering equipment, as an example, collectors of solar power, cooling devices of digital and micro-digital equipments and many others. Gill and Casal.^[8] have made an analysis on the influence of

electrically conducting the case of fully developed mixed convection between horizontal parallel plates with a linear axial temperature distribution. The problem of fully developed mixed convection between vertical plates with and without heat sources was solved by Ostrach.^[23] Cebeci et al.,^[5] performed numerical calculations of developing laminar mixed convection between vertical parallel plates for both cases of buoyancy aiding and opposing conditions. Al-Nimir and Haddad.^[3] have described the fully developed free convection in an open-ended vertical channel partially filled with porous material. Greif et al.^[9] have made an analysis on the laminar convection of a radiating gas in a vertical channel. Michael and Makinde.^[17] were described entropy generation in a variable viscosity channel flow of nano fluids with convective cooling.

Nanotechnology has been widely used in engineering and industry, since nanometer-sized materials possess unique physical and chemical properties. The addition of nanoscale particles into the conventional fluids like water, engine oil, ethylene glycol, etc., is known as nanofluid and was firstly introduced by Choi.^[6] Moreover, the effective thermal conductivity of conventional fluids increases remarkably with the addition of metallic nanoparticles with high thermal conductivity. Nanofluids may be considered as single phase flows in low solid concentration because of very small sized solid particles. There are many experimental and theoretical studies on the flow of nanofluids in different geometries (Abu-Nada,^[2] Choi et.al.^[7] Makinde,^[12] Makinde and Aziz,^[13] Makinde,^[14] Motsumi and Makinde.^[18] Mutuku-Njane and, Makinde,^[19] Olanrewaju and Makinde.^[22]). A numerical study of buoyancy-driven flow and heat transfer of an alu-mina (Al₂O₃)–water-based nanofluid in a rectangular cavity was done by Hwang et. al.^[10] The nanofluid in the enclosure was assumed to be in a single phase. It was found that for any given Grashof number, the average Nusselt number increased with the solid volume concentration parameter. Nield and Kuznetsov.^[21] investigated numerically the Cheng–Minkowycz problem for a natural convective boundary-layer flow in a porous medium saturated by a nanofluid. Oztop and Abu-Nada.^[24] considered natural convection in partially heated enclosures having different aspect ratios and filled with a nanofluid. They found that the heat transfer was more pronounced at low aspect ratios and high volume fractions of nanoparticles. Ibrahim and Makinde.^[11] studied the effect of double stratification on the boundary-layer flow and the heat transfer of nanofluid over a vertical plate. The buoyancy effects on the stagnation point flow and heat transfer of a nanofluid past a convectively heated stretching/shrinking sheet with or without magnetic field were considered by Makinde et. al.^[16] and Makinde.^[15] Wang and Mujumdar.^[26] presented a

comprehensive review of heat transfer characteristics of nanofluids. Detailed reports on convective transport in nanofluids can be found in Buongiorno,^[4] Mutuku-Njane and Makinde,^[19] Tiwari and Das.^[25] etc.

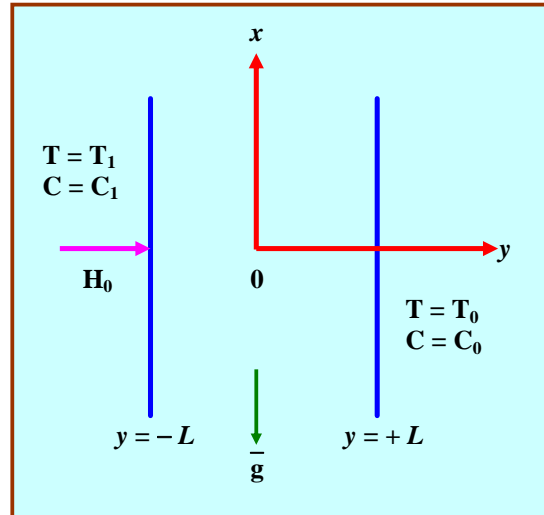


Fig.1. Schematic diagram of the problem under consideration

In the present study, we analyse the combined effects of thermophoresis, Brownian motion, activation energy and variable viscosity on the steady hydromagnetic channel flow of water-based nanofluid under the influence of irregular heat sources. Such flows are very important in engine cooling, solar water heating, cooling of electronics, cooling of transformer oil, improving diesel generator efficiency, cooling of heat exchanging devices, improving heat-transfer efficiency of chillers, domestic refrigerator and freezers, cooling in machining and in nuclear reactor. The governing equations have been solved by employing Runge-Kutta Fehlberg shooting method. In the following sections, the problem is formulated, numerically analysed, and solved. Pertinent results are displayed graphically and discussed.

2. Formulation of the Problem

Consider the steady flow of an electrically conducting, viscous fluid in a vertical channel by flat walls. A uniform magnetic field of strength H_0 is applied normal to the walls. Assuming the magnetic Reynolds number to be small we neglect the induced magnetic field in comparison to the applied field. The walls are maintained at constant temperatures T_1, T_2 and concentration C_1, C_0 . We consider a rectangular Cartesian coordinate system $O(x, y)$ with x -axis along the walls and y -axis normal to the walls. The walls are taken at $y = \pm L$. The boundary layer equations of flow, heat and mass transfer under Boussinesq approximation, and following Buongiorno model [2006] are:

Continuity

$$\frac{\partial u}{\partial x} = 0 \quad (1)$$

Momentum equation

$$0 = -\frac{\partial p}{\partial x} + \frac{\partial}{\partial y}(\mu_f(T)\frac{\partial u}{\partial y}) - \frac{\sigma B_o^2}{\rho_f}u + g[(1-C_o)\beta\rho_{f_0}(T-T_0) - (\rho_p - \rho_{f_0})(C-C_0)] \quad (2)$$

Energy equation

$$0 = \alpha_f \frac{\partial^2 T}{\partial y^2} + \tau(D_B \frac{\partial T}{\partial y} \frac{\partial C}{\partial y} + (\frac{D_T}{T_m})(\frac{\partial T}{\partial y})^2) + \frac{q'''}{\rho C_p} \quad (3)$$

Diffusion equation

$$0 = D_B \frac{\partial^2 C}{\partial y^2} + (\frac{D_T}{T_m}) \frac{\partial^2 T}{\partial y^2} - k_c(C-C_o)(\frac{T}{T_0})^n \text{Exp}(-\frac{E_n}{kT}) \quad (4)$$

The boundary conditions relevant to the problem are

$$\begin{aligned} u(-1) = 0, T = T_1, C = C_1 \quad \text{on } y = -L \\ u(+1) = 0, T = T_0, C = C_0 \quad \text{on } y = +L \end{aligned} \quad (5)$$

The internal heat generation or absorption term q''' (Eladhab and Aziz [2000]) is middled according to the following equation

$$q''' = \frac{k_f}{L^2} [A_{11}(T_1 - T_0)f' + B_{11}(T - T_0)]$$

Where A_{11} and B_{11} are the coefficient of space and temperature dependent heat source/sink respectively. It is to be noted that the case $A_{11} > 0$, $B_{11} > 0$ corresponds to internal heat generation while $A_{11} < 0$, $B_{11} < 0$, corresponds to internal heat absorption. The dynamic viscosity of the nanofluids is assumed to be temperature dependent as follows:

$$\mu_f(T) = \mu_o \text{Exp}(-m(T - T_0)) \quad (6)$$

where μ_o is the nanofluid viscosity at the ambient temperature T_0 .

m is the viscosity variation parameter which depends on the particular fluid.

Introducing non-dimensional variables as

$$\eta = \frac{y}{L}, u' = \frac{uL}{\mu_o}, \theta = \frac{T - T_0}{T_1 - T_0}, \phi = \frac{C - C_0}{C_1 - C_0}, p' = \frac{pL^2}{\mu_o^2} \quad (7)$$

The equations (2-4) reduce to

$$\frac{d^2 u'}{d\eta^2} - B \frac{du'}{d\eta} \frac{d\theta}{d\eta} + e^{b\theta} (A - M^2 u' + Gr(\theta - Nr\phi)) = 0 \quad (8)$$

$$\frac{d^2\theta}{dy^2} + Nb \frac{d\theta}{dy} \frac{d\phi}{dy} + Nt \left(\frac{d\theta}{dy}\right)^2 + A_{11}f' + B_{11}\theta = 0 \quad (9)$$

$$\frac{d^2\phi}{dy^2} + \left(\frac{Nt}{Nb}\right) \frac{d^2\theta}{dy^2} - \gamma Sc(1+n\delta\theta) \text{Exp}\left(-\frac{E_1}{1+\delta\theta}\right) = 0 \quad (10)$$

The corresponding boundary conditions are

$$\begin{aligned} u(-1) &= 0, \theta(-1) = 1, \phi(-1) = 1 \\ u(+1) &= 0, \theta(+1) = 0, \phi(+1) = 0 \end{aligned} \quad (11)$$

where

$$\begin{aligned} Gr &= \frac{\beta g(T_1 - T_0)(1 - C_o)L^3}{\mu_o^2}, M = \frac{\sigma B_o^2 L^2}{\mu_o}, Nr = \frac{(\rho_p - \rho_{f_0})(C_1 - C_0)}{\beta(1 - C_o)(T_1 - T_0)}, B = m(T_1 - T_0), \\ Nb &= \frac{\tau D_B(C_1 - C_0)}{\alpha_f}, Nt = \frac{\tau D_T(T_1 - T_0)}{\alpha_f}, \theta_w = \frac{T_1}{T_0}, \delta = \theta_w - 1, E_1 = \frac{E_a}{k_f T_0}, Sc = \frac{\nu}{D_B} \end{aligned}$$

are the Grashof number(G), magnetic parameter(M), Buoyancy ratio(Nr), viscous parameter (B), Brownian motion parameter(Nb), thermophoresis parameter(Nt), temperature difference parameter(δ), activation energy parameter(E_1), Schmidt parameter(Sc).

3. Numerical Analysis

The coupled non-linear ODEs (8)-(10) along with the corresponding boundary conditions (Bcs) (11) are solved by employing the RKF algorithm with Mathematica software. The numerical solutions are carried out by choosing the step size $\Delta\eta=0.001$.

(i) The coupled non-linear system of equations was transformed into a set of first order Des.

$$f = f_1, f' = f_2, f'' = f_3, \theta = f_4, \theta' = f_5, \phi = f_6, \phi' = f_7$$

(ii) The system of first order Des are

$$f''' = (Bf_2f_4) - e^{Bf_4}(A - M^2f_1 + Gr(f_4 - Nr f_6))$$

$$\theta'' = -(Nbf_5f_7 + Ntf_5^2 + A11f_1 + B11f_4)$$

$$\phi'' = -\left(\frac{Nt}{Nb}\right)(f_4f_6 + Nt^2f_4^2) + \gamma Sc(1+n\delta f_4)e^{-E1/(1+\delta f_4)}$$

The boundary conditions are

$$f_1(\pm 1) = 0, f_4(-1) = 1, f_5(+1) = 0, f_6(-1) = 1, f_6(+1) = 0$$

(iii) Suitable guess values are chosen for unknown required Bcs.

(iv) RKF technique with shooting method is utilized for step by step integration with the assistance of Mathematica software.

4. Skin Friction, Nusselt and Sherwood Number

The quantities of physical interest in this analysis are the skin friction, coefficient C_f , local Nusselt number (Nu), local Sherwood number (Sh) which are defined as

$$C_f = \frac{2\tau_w}{\rho u_w^2}, Nu = \frac{xq_w}{\alpha_f(T_1 - T_o)}, Sh = \frac{xm_w}{D_B(C_1 - C_o)} \quad (12)$$

where

$$\tau_w = \mu \left(\frac{\partial u}{\partial y} \right)_{\eta=\pm 1}, q_w = k_{nf} \left(\frac{\partial T}{\partial y} \right)_{\eta=\pm 1}, m_w = D_B \left(\frac{\partial C}{\partial y} \right)_{\eta=\pm 1} \quad (13)$$

Substituting equation (13) into equation (12), we get

$$C_f = e^{-B\theta} \left(\frac{\partial u}{\partial y} \right)_{\eta=\pm 1}, Nu = - \left(\frac{\partial \theta}{\partial y} \right)_{\eta=\pm 1}, Sh = - \left(\frac{\partial \phi}{\partial y} \right)_{\eta=\pm 1} \quad (14)$$

5. RESULTS AND DISCUSSION

The aim of this analysis is to study the combined influence of Activation energy, Brownian motion and thermophoresis on convective heat transfer flow of nanofluid confined in a vertical channel in the presence of irregular heat source. The effect of pertinent parameters on flow characteristics have been studied, on solving the coupled non-linear governing equations by Runge-Kutta Shooting method.

Figs.2a-2c demonstrate the effect of Grashof number (G) and magnetic parameter (M) on the velocity, temperature and concentration from the graphical representations we find that the velocity, temperature accelerate while the nanoconcentration decelerates in the flow region with increasing values of G. This shows that an increase in G grows the thickness of the momentum, thermal boundary layers and decays solutal layer thickness. With higher the strength of the Lorentz force the velocity, nanoconcentration depreciate and temperature rises. Physically, a retarding force or drag force (Lorentz force) is generated due to the presence of a magnetic force. On the other hand, the heat measure enhances and the mass of the fluid are depicted in figures 2b&c.

The effect of viscosity parameter (B) and buoyancy ratio (Nr) on flow variables can be seen from figs.3a-3c. Higher the viscosity parameter (B) larger the velocity, temperature and smaller the nanoconcentration in the flow region. When the molecular buoyancy force dominates over the thermal buoyancy force the velocity, temperature experience

enhancement while nanoconcentration depreciates when the buoyancy forces are in the same direction.

Figs.4a-4c represent the effect of Brownian motion (N_b) and thermophoresis parameter(N_t) on flow variables. A rise in N_b and N_t leads to a growth in velocity, temperature while nanoconcentration grows with N_b and decays with N_t . Physically, thermophoretic force creates a rise in the flow region. Consequently, as N_t increases the thickness of the momentum, thermal become layers become thicker and solutal layer becomes thinner (figs.4a-4c).

The effect of space dependent/temperature dependent heat sources (A_{11}, B_{11}) on flow variables can be seen from figs.5a-5c and 6a-6c. From the profiles we find that the velocity temperature enhance with rising values of space dependent/generating heat source ($A_{11} > 0, B_{11} > 0$) and reduces with heat sink ($A_{11} < 0, B_{11} < 0$) (fig.5c & 6c)

Figs.9a-9c exhibits the effect of chemical reaction parameter(γ) of θ and C . From the graphs The velocity increases, temperature and actual nanoparticle concentration depreciate in the degenerating chemical reaction case. This may be attributed to the fact that an increase in $\gamma > 0$ leads to growth of momentum layer, thermal and solutal boundary layers become thinner. In generating chemical reaction case, velocity experiences enhancement, temperature and nanoparticle concentration depreciates in the flow region.

Figs.7a-7c exhibit the effect of temperature relative parameter(δ) and activation energy parameter(E_1) on flow variables. Increasing activation energy(E_1) leads to a fall in velocity, temperature and rises nanoconcentration in the flow region. The effect of temperature difference parameter(δ) is to reduce velocity, temperature and enhances nanoconcentration. This is due to the fact that an increase in temperature relative parameter(δ) leads to thinning of the thickness of the momentum and thermal and thickening of the solutal boundary layers.

Lesser the molecular diffusivity/larger the index parameter (n) larger the velocity, temperature and smaller the nanoconcentration (figs.8a-8c). Figs.8a-8c represent the effect of Schmidt parameter(Sc) and index (n) on the flow variables. From the profiles we find that higher the Schmidt parameter(Sc) smaller the velocity and larger the temperature the actual nanoparticle concentration. This implies an increase in Sc leads to a decay in momentum and

growth in thermal and solutal boundary layers. An increase in index(n) increases the velocity, reduces the temperature and nanoparticle concentration in the flow region.

Figs.9a-9c represent the effect of chemical reaction parameter(γ) on flow variables. From the profiles we find that velocity, temperature and nanoconcentration experience an enhancement in the degenerating/generating chemical reaction cases.

The skin friction factor(C_f), Nusselt (Nu)and Sherwood number (Sh)at the walls $\eta = \pm 1$ are exhibited in table.1. From the tabular values we observe that the skin friction(C_f) grows at both the walls with increasing values of G , B , Nr , Nb , Nt , Sc , δ , γ and n . Higher the Lorentz force/activation energy, smaller C_f on $\eta = \pm 1$. C_f enhances with higher values of space /temperature dependent heat source($A_{11}>0, B_{11}>0$), while it reduces with heat sink($A_{11}<0, B_{11}<0$) at both walls.

The rate of heat transfer(Nu) depreciates at $\eta=-1$ and enhances at $\eta=+1$ with rising values of G , M , B , Nr , Nb , Nt, δ and n . An increasing activation energy (E_1)enhances Nu while it reduces with Sc . The rate of heat transfer decays in degenerating chemical reaction case ($\gamma>0$) at $\eta = \pm 1$ while in the generating case, Nu reduces at $\eta=-1$ and enhances at $\eta=+1$.

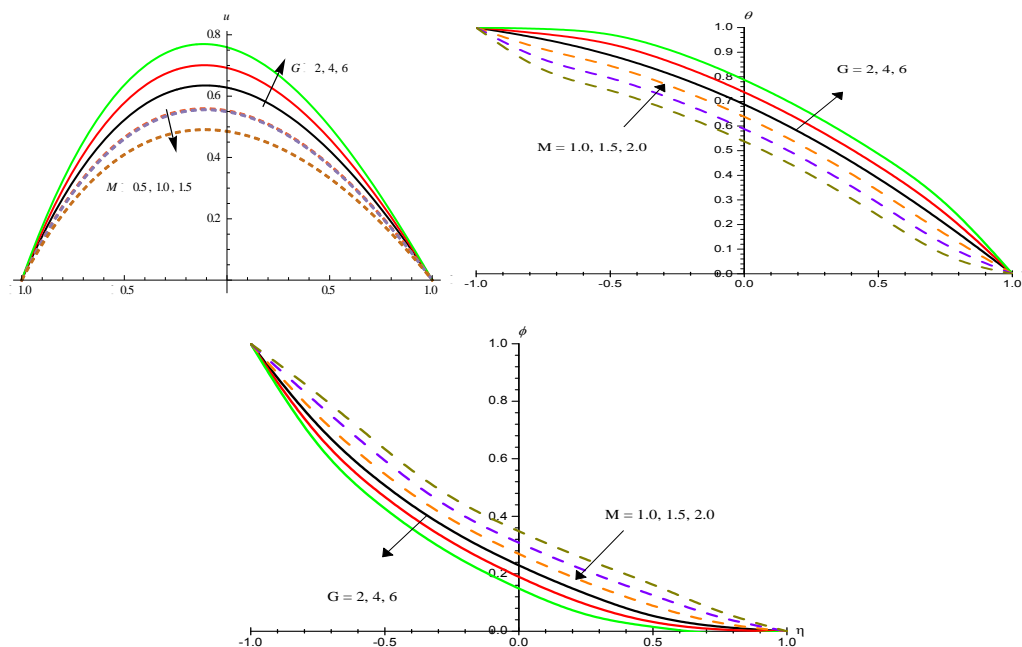


Fig. 2: Variation of [a] velocity(u), [b] Temperature(θ), nano-Concentration(ϕ) with G and M $Nr=0.2$, $B=0.3$, $Nb=0.2$, $Nt=0.1$, $A_{11}=0.2$, $B_{11}=0.2$, $E_1=0.1$, $\delta=0.2$, $Sc=0.24$, $n=0.2$, $\gamma=0.5$.

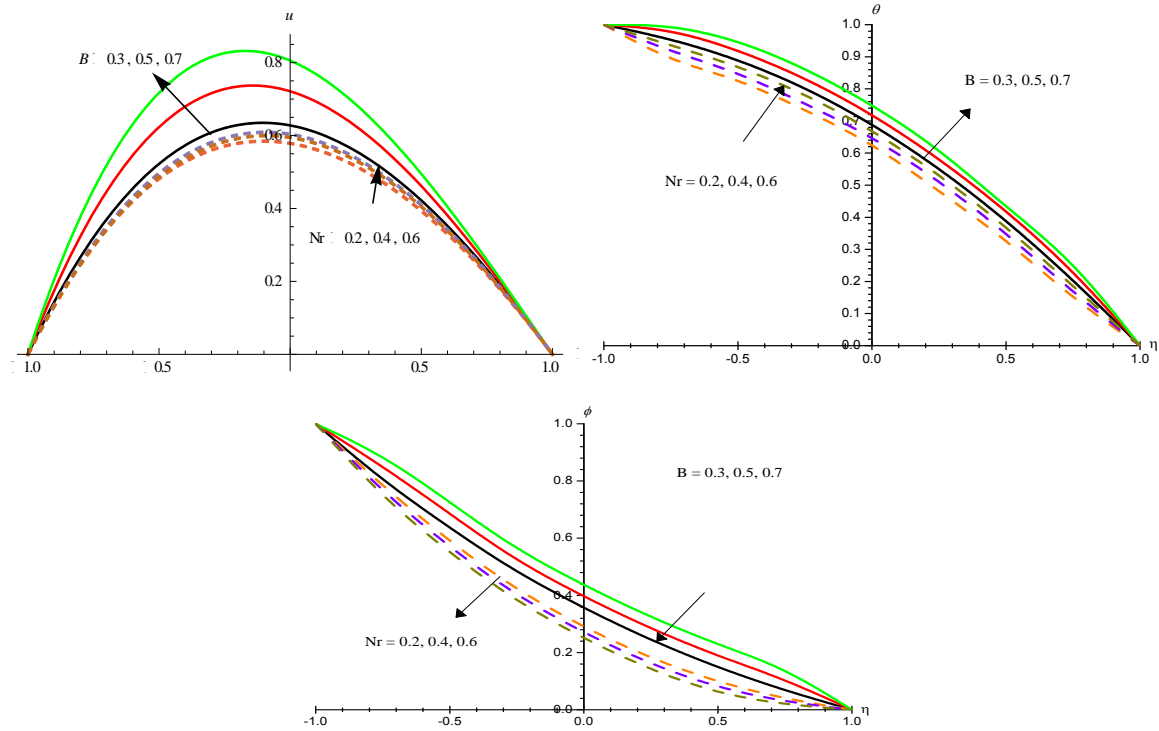


Fig. 3: Variation of [a] velocity(u), [b] Temperature(θ), nano-Concentration(ϕ) with Nr and B $G=2$, $M=0.5$, $Nb=0.2$, $Nt=0.1$, $A_{11}=0.2$, $B_{11}=0.2$, $E_1=0.1$, $\delta=0.2$, $Sc=0.24$, $n=0.2$, $\gamma=0.5$.

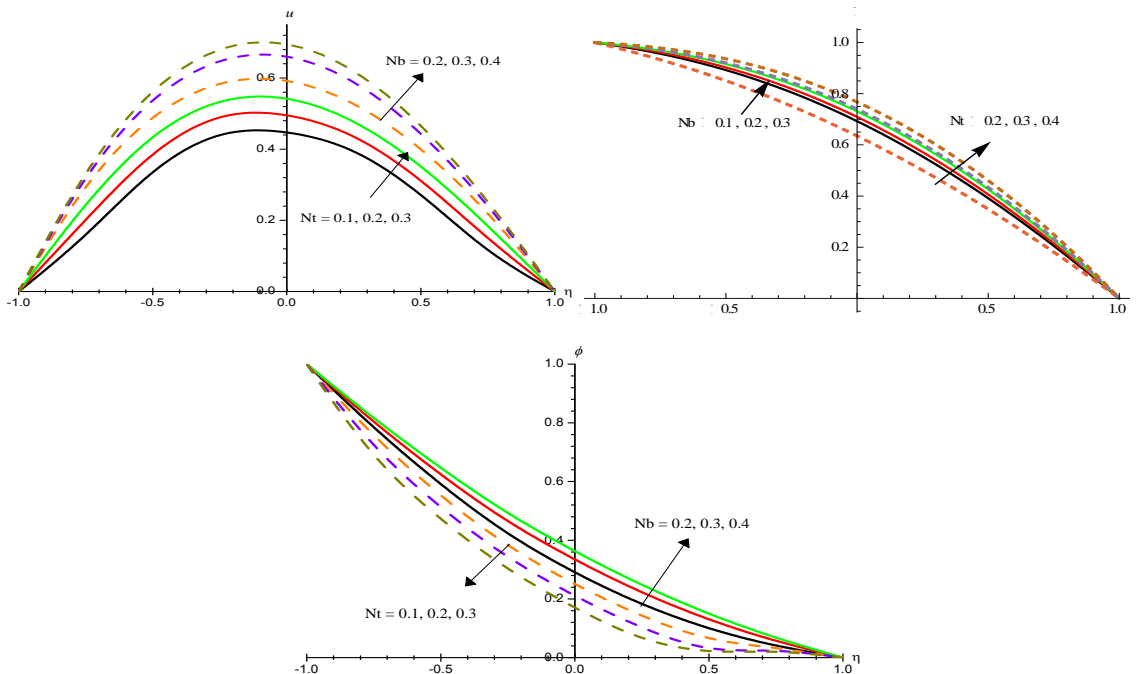


Fig. 4: Variation of [a] velocity(u), [b] Temperature(θ), nano-Concentration(ϕ) with Nb and Nt . $G=2$, $M=0.5$, $Nr=0.2$, $B=0.3$, $A_{11}=0.2$, $B_{11}=0.2$, $E_1=0.1$, $\delta=0.2$, $Sc=0.24$, $n=0.2$, $\gamma=0.5$.

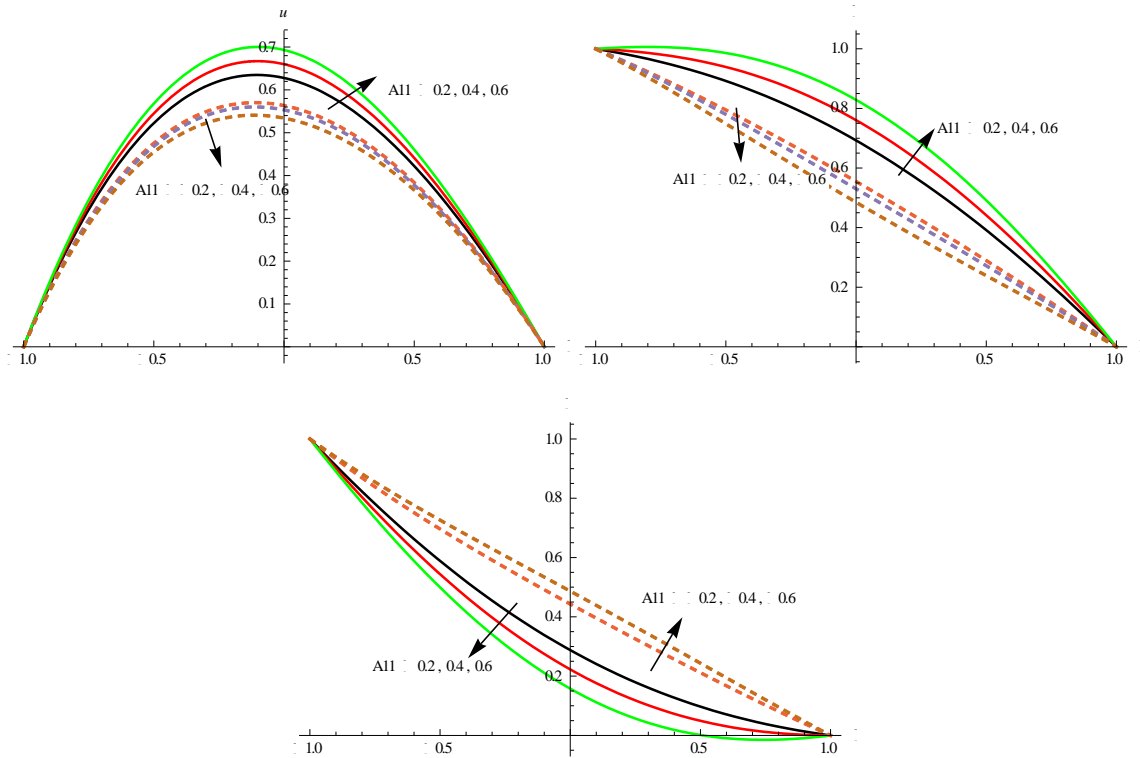


Fig. 5: Variation of [a] velocity(u), [b] Temperature(θ), nano-Concentration(ϕ) with $A11$ $G=2$, $M=0.5$, $Nr=0.2$, $B=0.3$, $Nb=0.2$, $Nt=0.1$, $B11=0.2$, $E1=0.1$, $\delta=0.2$, $Sc=0.24$, $n=0.2$, $\gamma=0.5$.

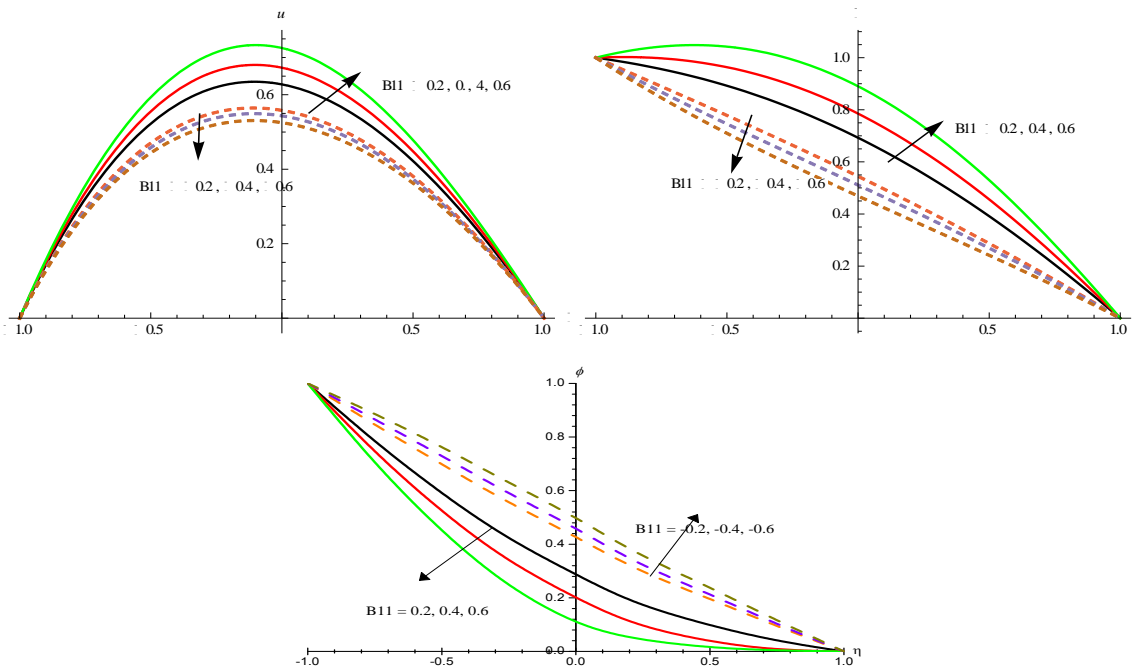


Fig. 6: Variation of [a] velocity(u), [b] Temperature(θ), nano-Concentration(ϕ) with $B11$ $G=2$, $M=0.5$, $Nr=0.2$, $B=0.3$, $Nb=0.2$, $Nt=0.1$, $A11=0.2$, $E1=0.1$, $\delta=0.2$, $Sc=0.24$, $n=0.2$, $\gamma=0.5$.

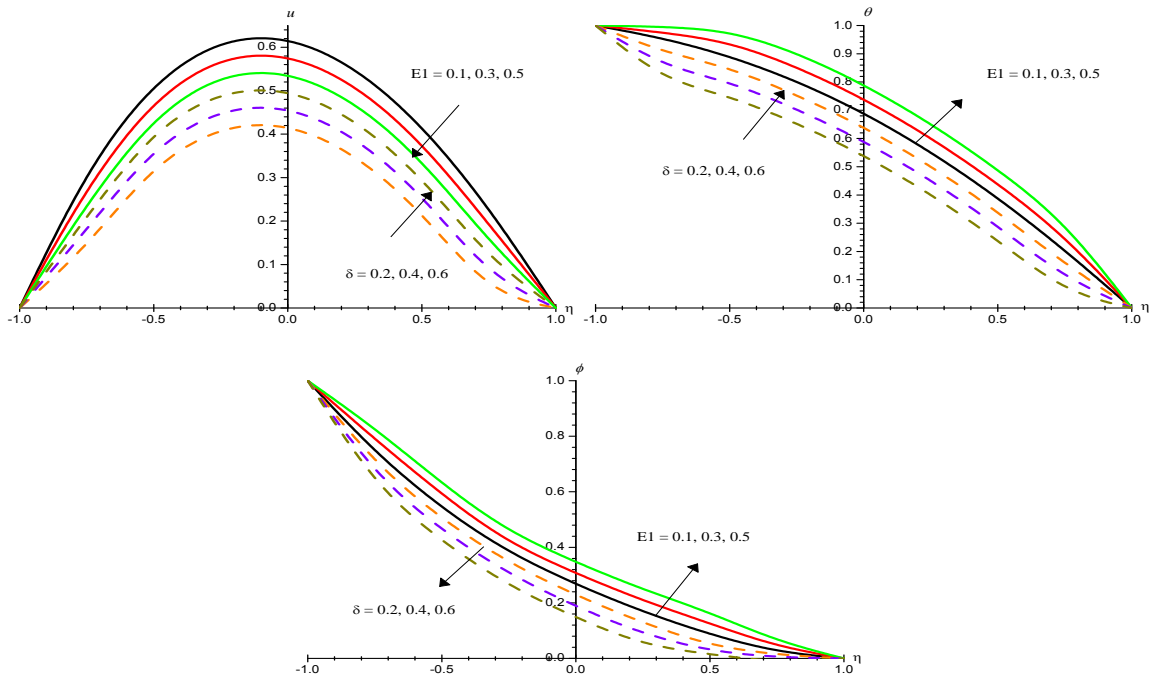


Fig. 7: Variation of [a] velocity(u), [b] Temperature(θ), nano-Concentration(ϕ) with $E1$ and δ . $G=2$, $M=0.5$, $Nr=0.2$, $B=0.3$, $Nb=0.2$, $Nt=0.1$, $A11=0.2$, $B11=0.2$, $Sc=0.24$, $n=0.2$, $\gamma=0.5$.

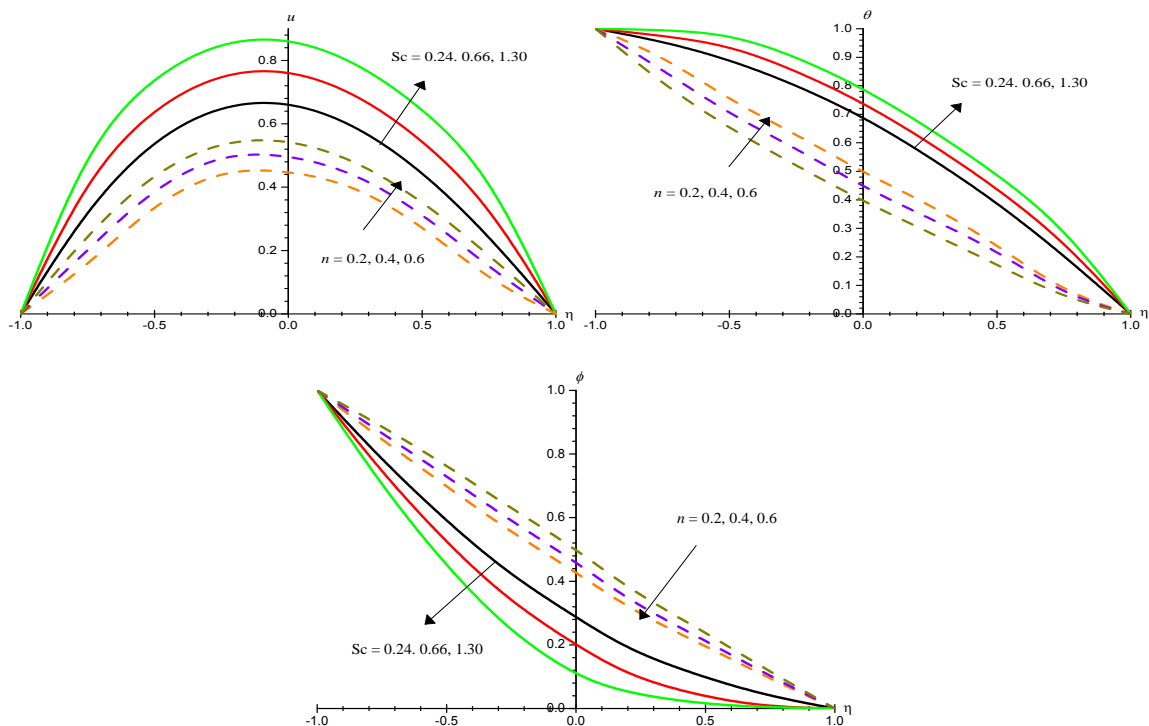


Fig. 8: Variation of [a] velocity(u), [b] Temperature(θ), nano-Concentration(ϕ) with Sc and n . $G=2$, $M=0.5$, $Nr=0.2$, $B=0.3$, $Nb=0.2$, $Nt=0.1$, $A11=0.2$, $B11=0.2$, $E1=0.1$, $\delta=0.2$, $\gamma=0.5$.

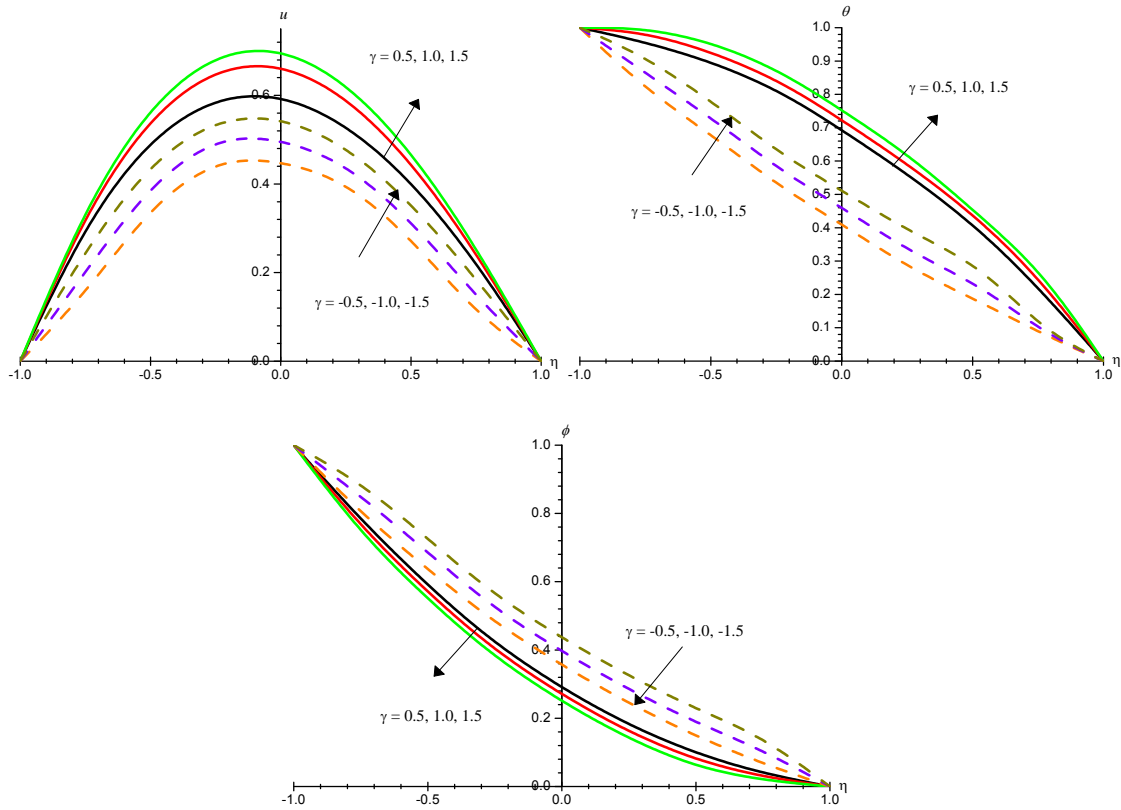


Fig. 9: Variation of [a] velocity(u), [b] Temperature(θ), nano-Concentration(ϕ) with γ $G=2$, $M=0.5$, $Nr=0.2$, $B=0.3$, $Nb=0.2$, $Nt=0.1$, $A11=0.2$, $B11=0.2$, $E1=0.1$, $\delta=0.2$, $Sc=0.24$, $n=0.2$.

Table 2: Skin-Friction(C_{fx}) and Nusslet(Nu) and Sherwood(Sh) Numbers at $\eta = \pm 1$.

Parameters		$\eta = -1$			$\eta = +1$		
		$C_{fx}(-1)$	$Nu(-1)$	$Sh(-1)$	$C_{fx}(+1)$	$Nu(+1)$	$Sh(+1)$
G	2	1.54282	0.14162	0.92367	-1.0083	0.85706	0.11955
	4	1.70514	0.13301	0.9319	-1.0829	0.86673	0.11027
	6	1.87275	0.12404	0.94047	-1.1608	0.87683	0.10058
M	0.5	1.41907	0.26384	0.80628	-0.9258	0.71625	0.2554
	1.0	1.39508	0.15153	0.87142	-0.9115	0.7853	0.20086
	1.5	1.27412	0.15965	0.90647	-0.8312	0.83563	0.14014
Nr	0.2	1.43987	0.26183	0.8082	-0.9628	0.71871	0.25304
	0.4	1.44671	0.16532	0.8592	-0.9853	0.78534	0.12905
	0.6	1.45083	0.14667	0.91883	-0.9992	0.85211	0.1243
B	0.3	1.54282	0.14162	0.92367	-1.0083	0.85706	0.11955
	0.5	1.88992	0.1276	0.93711	-1.0383	0.87008	0.10711
	0.7	2.22039	0.1147	0.94947	-1.0602	0.88172	0.09597
A11	0.2	1.54282	0.14162	0.92367	-1.0083	0.85706	0.11955
	0.4	1.58136	0.07421	1.01859	-1.0354	0.97531	0.006
	0.6	1.61989	0.05695	1.113	-1.0624	1.09339	0.10726
	-0.2	1.45866	0.3652	0.70918	-0.9507	0.60615	0.36119
	-0.4	1.44599	0.38073	0.69507	-0.9416	0.57419	0.39164

Parameters		$\eta = -1$			$\eta = +1$		
		Cfx(-1)	Nu(-1)	Sh(-1)	Cfx(+1)	Nu(+1)	Sh(+1)
	-0.6	1.42083	0.44784	0.63078	-0.9237	0.49516	0.46776
B11	0.2	1.54282	0.14162	0.92367	-1.0083	0.85706	0.11955
	0.4	1.59737	-0.0854	1.10411	-1.0454	1.00676	-0.1238
	0.6	1.65852	-0.0245	1.29582	-1.0873	1.17959	-0.1892
	-0.2	1.45032	0.44447	0.63098	-0.9465	0.60343	0.36335
	-0.4	1.42939	0.55346	0.52448	-0.9337	0.57509	0.38974
	-0.6	1.40398	0.66199	0.41885	-0.917	0.51242	0.44979
E1	0.1	1.54282	0.14162	0.92367	-1.0083	0.85706	0.11955
	0.3	1.54213	0.14171	0.91271	-1.0079	0.85761	0.12292
	0.5	1.54161	0.14177	0.90431	-1.0076	0.85802	0.12551
δ	0.2	1.4975	0.2602	0.82244	-0.9778	0.71976	0.24821
	0.4	1.53747	0.14183	0.94707	-1.0059	0.85565	0.11422
	0.6	1.53809	0.14177	0.95827	-1.0062	0.86517	0.11655
Nb	0.2	1.54282	0.14162	0.92367	-1.0083	0.85706	0.11955
	0.3	1.5431	0.11926	0.83461	-1.0089	0.90232	0.19255
	0.4	1.5443	0.09203	0.77547	-1.0092	0.9638	0.23907
Nt	0.1	1.51387	0.24231	0.93412	-0.99	0.74947	0.11932
	0.3	1.6081	0.08346	1.41712	-1.0601	0.98995	-0.529
	0.5	1.65919	0.05217	1.76395	-1.1005	1.07719	-1.0786
Sc	0.24	1.54238	0.14167	0.91597	-1.0081	0.8574	0.12142
	0.66	1.54741	0.14106	0.9982	-1.0108	0.85346	0.09733
	1.30	1.55185	0.14056	1.0738	-1.0131	0.85004	0.07698
n	0.2	1.4964	0.26039	0.80386	-0.9773	0.72022	0.25333
	0.4	1.53594	0.142	0.91965	-1.0052	0.85683	0.12083
	0.6	1.53605	0.14198	0.92159	-1.0052	0.85699	0.12036
γ	0.5	1.54238	0.14167	0.91597	-1.0081	0.8574	0.12142
	1.0	1.54693	0.14112	0.99022	-1.0105	0.85383	0.09958
	1.5	1.55165	0.14058	1.0703	-1.013	0.8502	0.07788
	-0.5	1.48742	0.26208	0.67238	-0.972	0.72415	0.30445
	-1.0	1.52942	0.14284	0.69507	-1.0016	0.86213	0.25407
	-1.5	1.52404	0.14157	0.73254	-1.0022	0.8666	0.18286

The rate of mass transfer(Sh)enhances at $\eta=-1$ and reduces at $\eta=+1$,with increasing values of G,M,B,Nr,Sc and n.A rise in Nb and E1 reduces Sh at $\eta=-1$ and grows at $\eta=+1$.Sh upsurges with Nt and δ at both the walls. Also Sh enhances at $\eta=-1$ and reduces at $\eta=+1$ with $\gamma>0$ while for $\gamma<0$,Sh enhances at both the walls. In addition, AE(E1) plays an important role in increasing the local heat transfer coefficient. Generally, AE is the minimum amount of energy that is required for a chemical reaction to stimulates atoms or molecules in the reaction. There should a considerable number of atoms whose AE is less than or equal to translational energy in a chemical reaction, hence in many engineering applications, AE may be considered as a better coolant.

6. CONCLUSIONS

The effect of irregular heat sources, variable viscosity and activation energy on flow characteristics in a vertical channel is analysed. The conclusions of this analysis are

- i) An increase in viscosity parameter (B) enhances the velocity, temperature and reduces nanoparticle concentration. The skin friction, Nusselt number grows, Sherwood number reduces with B at the left wall and an opposite effect is observed at the right wall.
- ii) Velocity and temperature reduces with $E1$ and depreciates with δ . Nanoconcentration augments with $E1$ and decays with δ . Nu enhances at both the walls with $E1$. Sh reduces at left wall and enhances at the right wall with $E1$.
- iii) Lesser molecular diffusivity larger velocity and temperature, Concentration reduces with Sc . Nu reduces with Sc .
- iv) Velocity, temperature and nanoconcentration enhances in both degenerating/generating chemical reaction cases. Nu reduces at the left wall and reduces at the right wall in the degenerating chemical reaction case.
- v) The velocity, temperature increase nanoparticle concentration reduces with increase in the strength of the space dependent heat source ($A11 > 0$). Cf , Nu and Sh increase with $A11$ and $B11$.

7. REFERENCES

1. Abo-Eldahab E. M. Abd El Aziz M. Hall and ion-slip effect on MHD free convective heat generating flow past a semi-infinite vertical flat plate *Phs. Scripta*, 2000; 61: 344.
2. Abu-Nada E., Application of nanofluids for heat transfer enhancement of separated flows encountered in a backward facing step, *Int. J. Heat Fluid Flow*, 2008; 29: 242–249.
3. Al-Nimir, M.A., Haddad, O. H: Fully developed free convection in open-ended vertical channels partially filled with porous material, *Journal Porous Media*, 1999; 2: 179-189.
4. Buongiorno J., Convective transport in nanofluids, *J. Heat Transf*, 2006; 128: 240–250.
5. Cebeci, T, Khattab, A. A and LaMont, R: Combined natural and forced convection in a vertical ducts, in: *Proc. 7th Int. Heat Transfer Conf.*, 1982; 3: 419-424.
6. Choi S.U.S., Enhancing thermal conductivity of fluids with nanoparticles, in: *Proc. ASME Int. Mech. Eng. Congress and Exposition*, ASME, San Francisco, USA, 1995; 99–105. FED 231/MD 66.
7. Choi S.U.S., Zhang Z.G., Yu W., Lockwood F.E., Grulke E.A., Anomalous thermal conductivity enhancement in nanotube suspensions, *Appl. Phys. Lett.*, 2001; 79(2): 2252–2254.

8. Gill, W.N. and Del Casal, A: A theoretical investigation of natural convection effects in forced horizontal flows, *AICHE J*, 1962; 8: 513-518.
9. Greif, R., Habib, I.S and Lin, J.C: Laminar convection of a radiating gas in a vertical channel, *J. Fluid. Mech.*, 1971; 46: 513.
10. Hwang K.S., Lee J.-H., Jang S.P., Buoyancy-driven heat transfer of water-based Al₂O₃nanofluids in a rectangular cavity, *Int. J. Heat Mass Transf*, 2007; 50: 4003–4010.
11. Ibrahim W., Makinde O.D., The effect of double stratification on boundary-layer flow and heat transfer of nanofluid over a vertical plate, *Comput. Fluids*, 2013; 86: 433–441.
12. Makinde O.D., Analysis of Sakiadis flow of nanofluids with viscous dissipation and Newtonian heating, *Appl. Math. Mech*, 2012; 33(12): 1545–1554.
13. Makinde O.D., Aziz A., Boundary layer flow of a nanofluid past a stretching sheet with a convective boundary condition, *Int. J. Therm. Sci.*, 2011; 50: 1326–1332.
14. Makinde O.D., Computational modelling of nanofluids flow over a convectively heated unsteady stretching sheet, *Curr. Nanosci*, 2013; 9: 673–678.
15. Makinde O.D., Effects of viscous dissipation and Newtonian heating on boundary layer flow of nanofluids over a flat plate, *Int. J. Numer. Methods Heat Fluid Flow*, 2013; 23(8): 1291–1303.
16. Makinde O.D., Khan W.A., Khan Z.H., Buoyancy effects on MHD stagnation point flow and heat transfer of a nanofluid past a convectively heated stretching/shrinking sheet, *Int. J. Heat Mass Transf*, 2013; 62: 526–533.
17. Michael Hamza Mkwizu, Oluwole Daniel Makinde Entropy generation in a variable viscosity channel flow of nano fluids with convective cooling, *Comptes Rendus Mecanique*, 2015; 343: 38–56. <http://dx.doi.org/10.1016/j.crme.2014.09.002>, www.sciencedirect.com.
18. Motsumi T.G., Makinde O.D., Effects of thermal radiation and viscous dissipation on boundary layer flow of nanofluids over a permeable moving flat plate, *Phys. Scr.*, 2012; 86: 045003.
19. Mutuku-Njane W.N., Makinde O.D., Combined effect of buoyancy force and Navier slip on MHD flow of a nanofluid over a convectively heated vertical porous plate, *Sci. World J.* 2013 (2013) 725643 (8pp.).
20. Mutuku-Njane W.N., Makinde O.D., MHD nanofluid flow over a permeable vertical plate with convective heating, *J. Comput. Theor. Nanosci.*, 2014; 11(3): 667–675.

21. Nield D.A., Kuznetsov A.V., The Cheng–Minkowycz problem for natural convective boundary-layer flow in a porous medium saturated by a nanofluid, *Int. J. Heat Mass Transf*, 2009; 52: 5792–5795.
22. Olanrewaju M., Makinde O.D., On boundary layer stagnation point flow of a nanofluid over a permeable flat surface with Newtonian heating, *Chem. Eng. Commun*, 2013; 200(6): 836–852.
23. Ostrach, S: Combined natural and forced convection laminar flow and heat transfer of fluid with and without heat sources in channels with linearly varying wall temperature, NACA TN, 1954; 3141.
24. Oztop H.F., Abu-Nada E., Numerical study of natural convection in partially heated rectangular enclosures filled with nanofluids, *Int. J. Heat Fluid Flow*, 2008; 29: 1326–1336.
25. Tiwari R.K., Das M.K., Heat transfer augmentation in a two-sided lid-driven differentially heated square cavity utilizing nanofluids, *Int. J. Heat Mass Transf.*, 2007; 50: 2002–2018.
26. Wang X.Q., Mujumdar A.S., Heat transfer characteristics of nanofluids: a review, *Int. J. Therm. Sci.*, 2007; 46: 1–19.